

## Studies of $^{54,56}\text{Fe}$ Neutron Scattering Cross Sections

S. F. Hicks<sup>1,a</sup>, J. R. Vanhoy<sup>2</sup>, A. J. French<sup>1</sup>, S. L. Henderson<sup>1</sup>, T. J. Howard<sup>1</sup>, R. L. Pecha<sup>1</sup>, Z. C. Santonil<sup>1</sup>, B. P. Crider<sup>3</sup>, S. Liu<sup>3</sup>, M. T. McEllistrem<sup>3,4</sup>, E. E. Peters<sup>4</sup>, F.M. Prados-Estévez<sup>3,4</sup>, T. J. Ross<sup>3,4</sup>, S.W. Yates<sup>3,4</sup>

<sup>1</sup>University of Dallas, Department of Physics, Irving, TX 75062, USA

<sup>2</sup>United States Naval Academy, Department of Physics, Annapolis, MD 21402, USA

<sup>3</sup>University of Kentucky, Department of Physics, Lexington, KY 40506

<sup>4</sup>University of Kentucky, Department of Chemistry, Lexington, KY 40506

**Abstract.** Elastic and inelastic neutron scattering differential cross sections and  $\gamma$ -ray production cross sections have been measured on  $^{54,56}\text{Fe}$  at several incident energies in the fast neutron region between 1.5 and 4.7 MeV. All measurements were completed at the University of Kentucky Accelerator Laboratory (UKAL) using a 7-MV Model CN Van de Graaff accelerator, along with the neutron production and neutron and  $\gamma$ -ray detection systems located there. The facilities at UKAL allow the investigation of both elastic and inelastic scattering with nearly mono-energetic incident neutrons. Time-of-flight techniques were used to detect the scattered neutrons for the differential cross section measurements. The measured cross sections are important for fission reactor applications and also for testing global model calculations such as those found at ENDF, since describing both the elastic and inelastic scattering is important for determining the direct and compound components of the scattering mechanism. The  $\gamma$ -ray production cross sections are used to determine cross sections to unresolved levels in the neutron scattering experiments. Results from our measurements and comparisons to model calculations are presented.

## 1 Introduction

The design and implementation of next-generation fission reactors is important for meeting our long-term energy needs. Neutron elastic and inelastic scattering cross sections for materials used in the reactor environment are important for designs that most efficiently produce nuclear power safely. There is currently a dearth of cross sections for many materials of interest in the fast neutron region, including cross sections for  $^{nat}\text{Fe}$  and Fe isotopes which are ubiquitous in structural materials.

Data evaluations are used to supply the needed cross sections to design engineers, but often the models used to determine the evaluations are based on experimental measurements that have large or non-existent uncertainties, little information on corrections for finite-sample effects, and/or the incident neutron energies represented in the existing data are sparse and, in many cases, non-existent for inelastic neutron scattering. Neutron inelastic scattering cross sections are very

important for determining the direct component of the reaction mechanism. Cross sections that are most needed for fission reactor design have been tabulated [1]. To provide neutron cross sections in the fast neutron energy region, a series of new neutron scattering measurements have been made at the University of Kentucky and are discussed here.

## 2 Experimental Apparatus and Techniques

Measurements were made at UKAL using the neutron production and detection and the  $\gamma$ -ray detection facilities located there. Protons or deuterons were accelerated using a 7 MV CN Van de Graaff accelerator, chopper, and bunching system to produce a 1.875 MHz pulsed beam that was bunched to  $\approx 1$  ns. Neutrons were produced with either the  $^3\text{H}(p,n)^3\text{He}$  or  $^2\text{H}(d,n)^3\text{He}$  source reactions. Neutron time-of-flight (TOF) techniques were used to

<sup>a</sup> Corresponding author: [hicks@udallas.edu](mailto:hicks@udallas.edu)

detect the scattered neutrons for the neutron measurements and to eliminate neutron background for the  $\gamma$ -ray detection measurements. Pulse-shape discrimination was used to reduce  $\gamma$ -ray background in the neutron measurements.

## 2.1 Neutron scattering differential cross sections

Enriched  $^{54}\text{Fe}$  (97.2%) and natural Fe samples were used to measure neutron scattering differential cross sections at seven incident neutron energies for  $^{\text{nat}}\text{Fe}$  and five incident neutron energies for  $^{54}\text{Fe}$ . An example neutron scattering TOF spectrum is shown in Fig. 1. A second scintillation detector was used for relative normalization for the TOF measurements; it was kept at a fixed angle in the laboratory and monitored source neutron production. The efficiency of the neutron detector was measured in situ by looking at source neutrons; an efficiency spectrum is shown in Fig. 2.

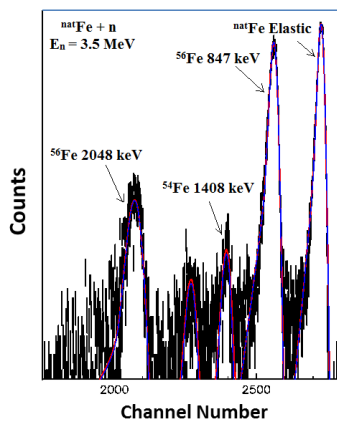


Figure 1. Neutron elastic scattering TOF spectrum at  $E_n = 3.50$  MeV from a  $^{\text{nat}}\text{Fe}$  sample. Scattering from  $^{54}\text{Fe}$  and  $^{56}\text{Fe}$  inelastic levels can be seen in the spectrum.

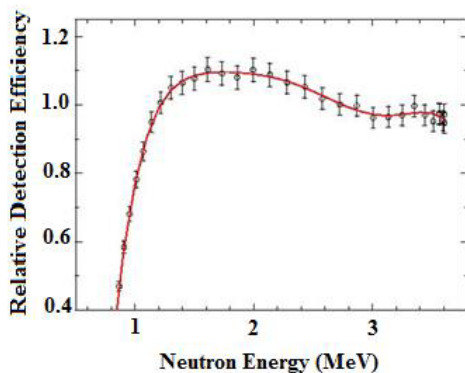


Figure 2. Relative detector efficiency of the neutron detector. The uncertainties in the  $^3\text{H}(p,n)^3\text{He}$  are the largest single contributor to the uncertainty at most angles.

Elastic and inelastic scattering differential cross sections were then deduced from the following expression,

$$\frac{d\sigma}{d\Omega} = \frac{N_{\text{abs}} Y_{\text{main}}}{Y_{\text{monitor}} \text{Eff}(E_n)} \quad (1)$$

where  $N_{\text{abs}}$  is the absolute normalization factor determined by comparing measured  $np$  scattering cross sections with the neutron scattering standard values;  $Y_{\text{main}}$  is the main detector yield;  $Y_{\text{monitor}}$  is the monitor detector yield; and  $\text{Eff}(E_n)$  is the neutron detection efficiency at energy  $E_n$ . The deduced cross sections were corrected for multiple scattering and neutron attenuation using MULCAT [2]. The multiple scattering corrections are estimated to be 10% of the correction based on input-parameter tests; these uncertainties are included in Figs. 5 and 6.

## 2.2 $\gamma$ -ray production cross sections

Gamma-ray excitation functions were measured on  $^{54}\text{Fe}$  and  $^{\text{nat}}\text{Fe}$  and on  $^{\text{nat}}\text{Al}$  and  $^{\text{nat}}\text{Ti}$  for  $E_n = 1.5 - 4.7$  MeV in 200 keV steps. These measurements were made to deduce neutron total inelastic cross sections for excited levels in  $^{56}\text{Fe}$  from  $\gamma$ -ray production cross sections. An example experimental  $\gamma$ -ray spectrum is shown in Fig. 3. The detection efficiency and the energy calibration of the HPGe detector used for the  $\gamma$ -ray measurements were determined using a  $^{226}\text{Ra}$  radioactive source.

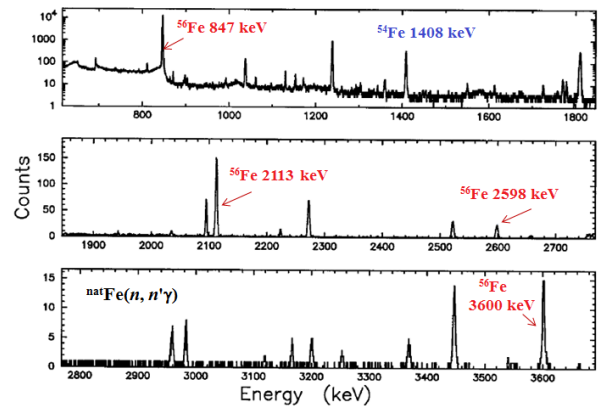


Figure 3. Gamma-ray spectrum on  $^{\text{nat}}\text{Fe}$ . Both  $^{54}\text{Fe}$  and  $^{56}\text{Fe}$  transitions are labeled.

Gamma rays were assigned to levels in  $^{54}\text{Fe}$  and  $^{56}\text{Fe}$  by comparing the shapes of the excitation functions, such as shown in Fig. 4. Branching ratios were also determined for each level; both the branching ratios and level assignments were compared to the adopted values from ENSDF [3].

## 3 Results and Conclusions

The  $^{56}\text{Fe}$  neutron total cross sections fluctuate over several barns near  $E_n = 1.75$  MeV [4]. Comparisons of new UKAL data to previous measurements near this energy by Smith et al. [4] show excellent agreement for the neutron elastic scattering differential cross sections, as can be seen in Fig. 5 and also with energy averaged ENDF evaluated data (not shown). For inelastic scattering, however, there is considerable deviation between the evaluated data and the UKAL data.

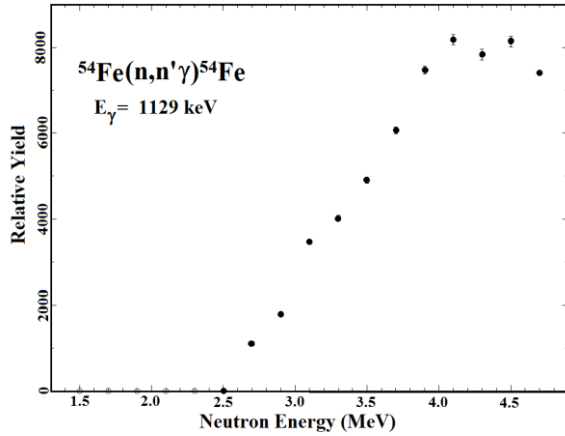


Figure 4. Example  $\gamma$ -ray excitation function for a transition from the 2538-keV excited level in  $^{54}\text{Fe}$ .

Figure 6 shows a comparison of these new data with several different evaluations; inelastic scattering experimental data do not previously exist at this incident neutron energy. Clearly, the models used for the evaluations do not well describe the neutron inelastic scattering at this energy.

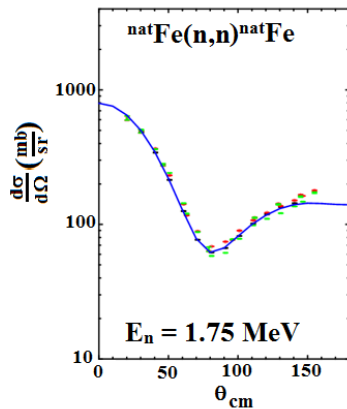


Figure 5. Comparison of UKAL data to previous measurements by Smith et al. [4]. The green and red data points are from Ref. [4] at  $E_n = 1.73$  MeV and 1.77 MeV, respectively. The solid line is the Legendre polynomial fit to the UKAL data at  $E_n = 1.75$  MeV.

Total neutron inelastic scattering cross sections were deduced from  $\gamma$ -ray production cross sections in  $^{56}\text{Fe}$ . Preliminary results for scattering from the  $2_1^+$  and  $4_1^+$  levels are shown in Fig. 7 in comparison to Ref. 5. The agreement is very good for the  $4_1^+$  state and within uncertainties for scattering from the  $2_1^+$  level at most energies.

In conclusion, the UKAL neutron scattering cross sections have revealed some discrepancies between evaluated neutron inelastic scattering data and experimental results, which are important for design considerations in fission reactors.

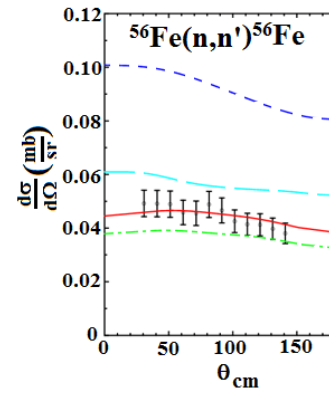


Figure 6. Neutron inelastic scattering differential cross sections at  $E_n = 1.75$  MeV compared to evaluated data from Ref. 4. (JENDL 2.0 MeV short-dashed blue; JENDL 1.0 long-dashed blue; ENDF 1.5 MeV red; ENDF 1.8 MeV dot-dashed green; UKAL data black)

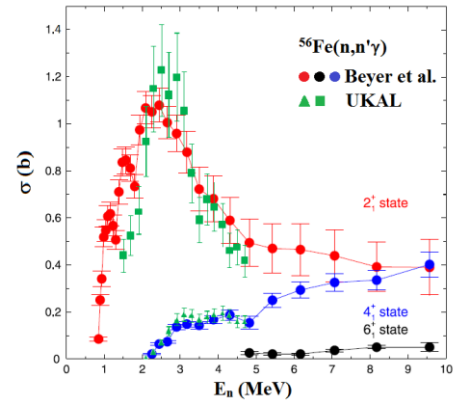


Figure 7. Comparison of neutron inelastic cross sections deduced from gamma-ray production cross sections. Green data are from UKAL and all others are from Beyer et al. [5]. UKAL data are preliminary.

## References

1. G. Aliberti, G. Palmiotti, M. Salvatores, C. G. Stenberg, Nucl. Science and Eng. **146**, 13 (2004); G. Aliberti, W.S. Yang, and R.D. McKnight, Nuclear Data Sheets **109**, 2745 (2008)
2. John R. Lilley, MULCAT-BRC, *A Monte Carlo Neutron and Gamma-Ray Multiple Scattering Correction Program*, Internal Service de Physique et Techniques Nucléaire, Centre d'Études de Bruyères-le-Châtel, Report P2N/934/80.(1980)
3. Evaluated Nuclear Structure Data File ( ENSDF) at [www.nndc.bnl.gov/ensdf/](http://www.nndc.bnl.gov/ensdf/)
4. Experimental Nuclear Reaction Data EXFOR/CSISRS at [www.nndc.bnl.gov](http://www.nndc.bnl.gov)
5. R. Beyer, R. Schwengner, R. Hannaske, A. R. Junghans, R. Massarczyk, M. Anders, D. Bemmerer, A. Ferrari, A. Hartmann, T. Kögler, M. Röder, K. Schmidt, A. Wagner, Nucl. Phys. A **927**, 41 (2014)

